ResearchGate

See discussions, stats, and author profiles for this publication at: https://www.researchgate.net/publication/220065812

Biped Hopping Control Bazsed on Spring Loaded Inverted Pendulum Model.

Article *in* International Journal of Humanoid Robotics · June 2010

DOI: 10.1142/S0219843610002106 · Source: DBLP

CITATIONS
26

READS
1,752

4 authors, including:

Seyed Hossein Tamaddoni
Virginia Polytechnic Institute and State University
18 PUBLICATIONS **157** CITATIONS
SEE PROFILE

Ali Meghdari
Sharif University of Technology
391 PUBLICATIONS **2,778** CITATIONS
SEE PROFILE

s. Sohrabpour
Sharif University of Technology
81 PUBLICATIONS **1,661** CITATIONS
SEE PROFILE

Some of the authors of this publication are also working on these related projects:

Utilizing Social Robots and Intelligent Devices in Rehabilitation of Children with Autism in Iran View project

Patellofemoral Joint Biomechanics View project

All content following this page was uploaded by Ali Meghdari on 22 May 2014.

The user has requested enhancement of the downloaded file.

International Journal of Humanoid Robotics
Vol. 7, No. 2 (2010) 1–18
© World Scientific Publishing Company
DOI: 10.1142/S0219843610002106

World Scientific
www.worldscientific.com

BIPED HOPPING CONTROL BASED ON SPRING LOADED INVERTED PENDULUM MODEL

SEYED HOSSEIN TAMADDONI*, FARID JAFARI†,
ALI MEGHDARI‡ and SAEED SOHRABPOUR§

Center of Excellence in Design,
Robotics, and Automation (CEDRA),
School of Mechanical Engineering,
Sharif University of Technology, Tehran, Iran
**h.tamaddoni@gmail.com*
†*jafari.farid@gmail.com*
‡*meghdari@sharif.edu*
§*sohrabpour@sharif.edu*

Received
Revised
Accepted

Human running can be stabilized in a wide range of speeds by automatically adjusting muscular properties of leg and torso. It is known that fast locomotion dynamics can be approximated by a spring loaded inverted pendulum (SLIP) system, in which leg is replaced by a single spring connecting body mass to ground. Taking advantage of the inherent stability of SLIP model, a hybrid control strategy is developed that guarantees a stable biped locomotion in sagittal plane. In the presented approach, nonlinear control methods are applied to synchronize the biped dynamics and the spring-mass dynamics. As the biped center of mass follows the mass of the mass-spring model, the whole biped performs a stable locomotion corresponding to SLIP model. Simulations are done to obtain a repeatable hopping for a three-link underactuated biped model. Results show that periodic hopping gaits can be stabilized, and the presented control strategy provides feasible gait trajectories for stance and swing phases.

Keywords: Biped; hopping; jumping; running; SLIP; gait; control.

1. Introduction

For decades, motion planning has been a crucial step in developing walking robots. In particular, there is significant interest on developing systematic methods of gait generation for biped robots.[1–4] Among the existing methods, the objective function oriented approach that regulates the motion of a planar link-segmental biped robot such that the cost is minimized has shown considerable advantages. Through this method, biped locomotion can be characterized in terms of step length, progression speed, maximum step height and the stance knee bias angle. According to the objective function, joint angular displacement profiles can be then uniquely determined based on the initial condition of the system.

Despite different gaits and speeds, human and legged animal fast locomotion can be described by spring-like leg behavior[5]; hence, fast locomotion including running, jumping, hopping, and etc. can be represented by a simple spring-mass system, known as *Spring Loaded Inverted Pendulum* or SLIP.[6,7] This model is based on observations which revealed that the energy level remains approximately constant during running, hopping and jumping. Associated with the spring-like leg behavior, *leg stiffness* is defined that is shown to remain almost constant during fast locomotion.[8] Thus, the spring-mass representation seems to provide acceptable insight to human fast locomotion.[9,10] It is also known that the spring-mass model is repeatable and self-stabilizing for adequate leg parameter adjustments, including angle of attack, leg stiffness, and leg length, and sufficient speeds.[8,11]

In this paper, a new approach to biped trajectory planning and control in hopping locomotion is introduced based on synchronization of biped governing dynamics and SLIP dynamics that corresponds to a particular hopping motion. This method is biologically inspired by the idea that biped must follow human trajectory which is considered an ideal self-stabilizing pattern in order to become capable of fast locomotion.[12,13]

A link-segmental model of the biped with three degrees of freedom and one degree of underactuation in the ankle joint is developed in this paper. Using the proposed control strategy, the biped joint torques are commanded such that the biped dynamics follows its corresponding SLIP model. Later discussed, the initial conditions are set in a way that a periodic hopping motion is achieved. Simulation results show a periodic hopping locomotion can be achieved using the proposed synchronization control method.

2. Dynamics Model of Hopping

The robot is assumed to consist of three rigid links with mass, connected via rigid, frictionless, revolute joints to for a single open kinematic chain lying in sagittal plane. The hopping occurs on a flat horizontal surface, thus without loss of generality it is assumed that the ground height is zero with respect to the inertial frame.

A complete cycle of hopping consists of two consecutive phases:

(1) *stance* in which leg end is in stationary contact with the ground and as an ideal pivot supports the whole body. If the biped center of mass (CoM) reaches a sufficient upward velocity, the leg loses its contact to the ground and the phase ends,
(2) *flight* in which there is no contact with the ground, and it ends as soon as a sudden impact with the ground surface occurs.

Figure 2 illustrates different phases of running with coordinate conventions of this paper labeled on a link-segmented model of biped robot in sagittal plane. The biped model in this study has three links each of which has length, mass, and moment

of inertia. There is one degree of underactuation in ankle joint of the biped, so the robot cannot apply any torque at its foothold.

Assuming that $\theta, \dot{\theta}, \ddot{\theta}$, and τ represent the generalized coordinates, velocities, accelerations, and torques, respectively, the dynamic model describing the motion of the biped in stance phase can be written as,[14]

$$D(\theta)\ddot{\theta} + C(\theta, \dot{\theta})\dot{\theta} + G(\theta) = B\tau \tag{1}$$

where $D(\theta)$ is the inertia matrix, $C(\theta, \dot{\theta})$ is the Coriolis matrix, $G(\theta)$ is the gravity vector, and B is the control matrix.

For $i, j = 1, 2, 3$, the matrices D, C, G are given by:

$$\begin{cases} D_{ij}(\theta) = \left(m_j d_j l_j + \left(\sum_{k=j+1}^{3} m_k \right) l_i l_j \right) \cos(\theta_i - \theta_j) \\ C_{ij}(\theta, \dot{\theta}) = \left(m_j d_j l_j + \left(\sum_{k=j+1}^{3} m_k \right) l_i l_j \right) \sin(\theta_i - \theta_j)\, \dot{\theta}_j \\ G_i(\theta) = \left(m_j d_j g + \left(\sum_{k=i+1}^{3} m_k \right) l_i g \right) \sin\theta_i \,. \end{cases} \tag{2}$$

Since the biped is underactuated in the contact point, no torque can be exerted from the ground to the first link. Therefore, the control matrix B corresponding to the generalized torque vector $\tau = [\tau_2 \quad \tau_3]^T$ is given by,

$$B = \begin{bmatrix} -1 & 0 \\ 1 & -1 \\ 0 & 1 \end{bmatrix} \tag{3}$$

During flight phase, five degrees of freedom including joint angles and ankle position are defined to describe the governing dynamics. The biped center of mass undergoes a ballistic trajectory, and the exerted torques in knee and hip defines the angle trajectory during flight. Given that the angle trajectories of ankle and knee joints are known, the hip angle and ankle position is determinant by flight dynamics.

When the ankle touches the ground at the end of flight phase, an impact takes place. Based on the existing impact models, the ground reaction forces at impact can be represented by impulses with intensity I_R. In this paper, the impact is assumed inelastic, and the velocity of the ankle becomes zero instantaneously. As a result of this model, the robot's configuration is assumed unchanged during impact and there are only instantaneous changes in the velocities.

The Cartesian position of the ankle can be expressed in terms of Cartesian position of biped center of mass as,

$$\begin{bmatrix} x_a \\ y_a \end{bmatrix} = \begin{bmatrix} x_c \\ y_c \end{bmatrix} - s(\theta) \tag{4}$$

where s is determined from the in-between link parameters such as length, mass, and position of center of mass.

Let $\dot{\theta}^-, \dot{\theta}^+$ denote the velocity vector just before and after the impact, respectively. After impact, the ankle neither rebounds nor slides; therefore, the linear velocity of the center of mass can be expressed in terms of the angular velocities just after impact as,

$$\begin{bmatrix} 0 \\ 0 \end{bmatrix} = \begin{bmatrix} \dot{x}_c^+ \\ \dot{y}_c^+ \end{bmatrix} - \frac{\partial s(\theta)}{\partial \theta} \dot{\theta}^+. \tag{5}$$

The ground reaction impulse vector is given by,

$$I_R = m \left(\frac{\partial s(\theta)}{\partial \theta} \dot{\theta}^+ - \begin{bmatrix} \dot{x}_c^- \\ \dot{y}_c^- \end{bmatrix} \right) \tag{6}$$

and the robot's angular velocity vector after impact is obtained with respect to the velocity before impact as,

$$\dot{\theta}^+ = \left(A(\tilde{\theta}) + m \frac{\partial s^T(\theta)}{\partial \theta} \frac{\partial s(\theta)}{\partial \theta} \right)^{-1} \begin{bmatrix} A(\tilde{\theta}) & m \frac{\partial s^T(\theta)}{\partial \theta} \end{bmatrix} \dot{\theta}^- \tag{7}$$

where $\tilde{\theta}$ is the relative angles of the actuated joints with reference to the biped body, and A is the matrix that defines the total kinetic energy of the robot during flight,

$$K_f = \frac{1}{2} \dot{\tilde{\theta}}^T A \dot{\tilde{\theta}} + \frac{1}{2} m (\dot{x}_c^2 + \dot{y}_c^2). \tag{8}$$

3. Spring Loaded Inverted Pendulum Model

The planar spring model is characterized by alternating stance and flight phases. Figure 1 illustrates the parameters of the spring mass model. The point mass m

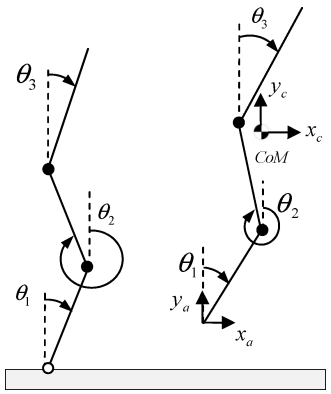

Fig. 1. Three-link model of biped robot.

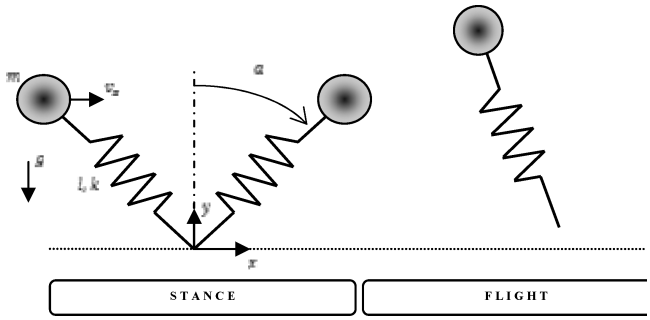

Fig. 2. Spring mass running model.

represents the effective body mass, which is supported by a linear spring of stiffness k and rest length l_0. During stance phase, the spring is pinned to the ground with the angle of attack α between the neutral axis and the point mass. During flight phase, the center of mass describes a ballistic curve, determined by the gravitational force acting downward.

The transition to stance phase occurs when the following landing condition is satisfied:

$$y = l_0 \sin(\alpha_{TD}) \tag{9}$$

where α_{TD} is the touch-down angle of attack.

During stance phase, spring mass dynamics is governed by spring forces and gravity, and the equation of motion is:

$$\begin{cases} m\ddot{l} = ml\dot{\alpha}^2 - mg\cos\alpha - k(l - l_0) \\ ml\ddot{\alpha} = -2m\dot{l}\dot{\alpha} + mg\sin\alpha \end{cases} \tag{10}$$

where l, l_0 are the spring current length and rest length, respectively, and α is the angle of attack.

Assuming small angle of attack, α, an approximated analytical solution can be obtained for the spring mass system of Eq. (2).[9] However, since biped hops in a wide range of angle of attacks, the equations of motion for spring mass system is solved numerically in this work.

During flight phase, the center of mass describes a ballistic curve, determined by the gravitational force acting downward:

$$\begin{cases} \ddot{x}_c = 0 \\ \ddot{y}_c = -g. \end{cases} \tag{11}$$

Combining equations (10) and (11), a hybrid model is formed that describes the dynamics of spring mass in stance and flight.

Since, the horizontal component of center of mass velocity, v_x, remains unchanged during flight phase, its value should be the same at touchdown and takeoff to guarantee periodicity of hopping motion. This implies that symmetry of

stance is a necessary condition for generating periodic motion; however, improved hopping performance usually involves asymmetric stance phase. Following Geyer *et al.*,[15] this dilemma is resolved in simulations by removing the symmetry condition of stance phase, and readjusting the horizontal component of velocity at touchdown for asymmetric stance.

Furthermore, SLIP dynamics becomes more flexible by assuming that the rest length of the spring is a function of angle of attack; this way, larger momentum can be achieved during stance which results in a longer hopping step size.

For spring mass system, cycle periodicity is characterized by fixed apex height h^* such that $h_i = h_{i+1} = h^*$ while horizontal velocity is maintained positive, $v_x > 0$. Also, stability of this system can be analyzed by one-dimensional return map of two subsequent apex heights. For stability analysis, the strength of attraction which is defined by the slope of the return map $h_{i+1}(h_i)$ as,

$$\eta = \left.\frac{dh_{i+1}}{dh_i}\right|_{h*} \tag{12}$$

should be within $(-1, +1)$ in the neighborhood of a fixed point $h*$ to guarantee stable movement.

4. Control Strategy

In this section, a control strategy is developed to generate a periodic, stable hopping motion for an underactuated three-link robot. During stance, a master-slave synchronization control strategy is applied, assuming mass spring and biped dynamics as the master and slave systems, respectively.[12,13] In flight phase, the joint trajectories of two lower links are designed using polynomial time functions such that the periodicity conditions are satisfied. To guarantee a periodic hopping, fixed points of the associated Poincare map are sought and the corresponding initial conditions are fed into the system.

4.1. *Stance control*

To synchronize the motion of the robot with the master dynamics of the SLIP model, the coordinates of the biped's center of mass (CoM) should be obtained in polar coordinate system. Assuming the coordinate origin at the foothold, the expression for these coordinates can simply be simplified by introducing the following metric:

$$q_{ij} = \begin{cases} d_j/M, & i = j \\ l_j/M, & i > j \\ 0, & i < j \end{cases} \tag{13}$$

where M is the total mass of the robot, and $i, j = 1, 2, 3$ are the link number.

This way, the Cartesian and polar coordinates of the CoM are consecutively given by

$$x_c = \sum_{i,j=1}^{3} m_i q_{ij} \sin\theta_j \tag{14}$$

$$y_c = \sum_{i,j=1}^{3} m_i q_{ij} \cos\theta_j \tag{15}$$

and,

$$\eta = \sqrt{x_c^2 + y_c^2} \tag{16}$$

$$\gamma = \tan^{-1}\left(\frac{x_c}{y_c}\right) \tag{17}$$

With κ being either of η and γ, double differentiating with respect to time yields

$$\ddot{\kappa} = \dot{\theta}^{\mathbf{T}} \frac{\partial^2 \kappa}{\partial \theta^2} \dot{\theta} + \frac{\partial \kappa}{\partial \theta} \ddot{\theta} \tag{18}$$

1 Here, $\partial\kappa/\partial\theta$ should be regarded as a row vector for the matrix operations to be proper.

From combining Eq. (1) with Eq. (18), it follows that

$$\begin{cases} \ddot{\eta} = f_\eta(\theta, \dot{\theta}) + g_\eta(\theta) B\tau \\ \ddot{\gamma} = f_\gamma(\theta, \dot{\theta}) + g_\gamma(\theta) B\tau \end{cases} \tag{19}$$

where

$$f_\kappa(\theta, \dot{\theta}) = \dot{\theta}^T \frac{\partial^2 \kappa}{\partial \theta^2} \dot{\theta} - \frac{\partial \kappa}{\partial \theta} D^{-1} \left(C\dot{\theta} + G \right) \tag{20}$$

$$g_\kappa(\theta) = \frac{\partial \kappa}{\partial \theta} D^{-1} \tag{21}$$

Synchronizing control design involves defining an error function as

$$e = \begin{Bmatrix} \eta - l \\ \gamma - \alpha \end{Bmatrix} \tag{22}$$

and asymptotically stabilizing it around zero. Based on the feedback linearization method of nonlinear control, a simple PD controller is considered with proportional gain, K_p, and differential gain,K_d. The control input can be obtained from the following equation:

$$\begin{bmatrix} g_\eta(\theta) \\ g_\gamma(\theta) \end{bmatrix} B\tau = K_p e + K_d \dot{e} + \begin{bmatrix} l\dot{\alpha}^2 - g\cos\alpha - \dfrac{k}{m}(l - l_0) - f_\eta(\theta, \dot{\theta}) \\ \dfrac{-2\dot{l}\dot{\alpha} + g\sin\alpha}{l} - f_\gamma(\theta, \dot{\theta}) \end{bmatrix} \tag{23}$$

Proper selection of the control gains, error function can be stabilized around zero; hence, it becomes:

$$\ddot{e} + K_d\dot{e} + K_p e = 0. \tag{24}$$

Since the biped is underactuated, the generalized torque vector could be fully determined by specifying the torque at knee and hip. From Eq. (23), it follows that

$$\tau = \begin{bmatrix}\tau_2\\ \tau_3\end{bmatrix} = \left(\begin{bmatrix}g_\eta(\theta)\\ g_\gamma(\theta)\end{bmatrix} B\right)^{-1}\left(K_p e + K_d\dot{e} + \begin{bmatrix}\ddot{l} - f_\eta(\theta,\dot{\theta})\\ \ddot{\alpha} - f_\gamma(\theta,\dot{\theta})\end{bmatrix}\right) \tag{25}$$

where the control matrix B was defined in Eq. (3).

Equation (25) is valid for nonzero determinant of the inverted matrix. It can be shown that singularity condition of this matrix is equivalent to the following:

$$\begin{vmatrix} & g_\eta(\theta) & \\ & g_\gamma(\theta) & \\ 1 & 1 & 1\end{vmatrix} = 0. \tag{26}$$

There is no general condition on system nonsingularity; however, no singularity is expected to occur due to the form of $g_\eta(\theta)$ and $g_\gamma(\theta)$ that is defined in this paper for hopping.

4.2. *Flight control*

Throughout flight, the biped center of mass undergoes a ballistic trajectory which is solely determined by gravitational acceleration and the initial conditions — the takeoff conditions in the case of hopping and jumping. In this phase, the biped system has five degrees of freedom: three joint angles and two other coordinates locating the biped in x–y coordinates. In this paper, the latter two states are selected to be the coordinates showing the biped ankle position.

A periodic solution is the one in which the state variables at each touchdown satisfy certain conditions presented below:

$$\begin{aligned}\theta_i^n &= \theta_i^{n+1} \quad i = 1,2,3\\ \dot{\theta}_i^n &= \dot{\theta}_i^{n+1} \quad i = 1,2,3.\end{aligned} \tag{27}$$

One common method of planning such trajectory is solving an optimization problem to minimize or even nullify the error defined by the difference between the states at two consecutive touchdowns. However, in this paper, the joint space trajectory is passively generated so that the periodicity conditions are satisfied. For this purpose, it is first noticed that there are two input torques that control the system configuration. Based on the limited number of control input, only two joint profiles can be determined, which are the shank and thigh joints in this paper. The profiles of these angles are separately interpolated by third degree polynomials

between any takeoff and the next touchdown. The periodicity conditions of Eq. (27) can be rewritten as,

$$\begin{cases} \theta_i(t_{TO_n}) = \theta_i^{TO_n} \\ \dot{\theta}_i(t_{TO_n}) = \theta_i^{TO_n} \\ \theta_i(t_{TD_n}) = \theta_i^{TD_{n-1}} \\ \dot{\theta}_i(t_{TD_n}) = (\dot{\theta}_i^{TD_{n-1}})^- \end{cases}, \quad i = 1, 2 \tag{28}$$

where the indices TO and TD correspond to takeoff and touchdown, respectively.

The equations of motion, could again be written in a matrix form similar to Eq. (1), in which θ_1 and θ_2 are known from the polynomial interpolations, therefore, leaving three other states, θ_3, x_a, and y_a, to be determined. Since these coordinates are governed by flight dynamics, they can be separated from the two previously determined variables resulting in a simplified form of equations of motion as,

$$\begin{bmatrix} D_{11} & D_{12} \\ D_{21} & D_{22} \end{bmatrix} \begin{bmatrix} \ddot{X}_1 \\ \ddot{X}_2 \end{bmatrix} + \begin{bmatrix} N_1 \\ N_2 \end{bmatrix} = \begin{bmatrix} -\tau_2 \\ \tau_2 - \tau_3 \\ \tau_3 \\ 0 \\ 0 \end{bmatrix} \tag{29}$$

where $X_1 = \begin{bmatrix} \theta_1 & \theta_2 \end{bmatrix}^T$ is known and $X_2 = \begin{bmatrix} \theta_3 & x_a & y_a \end{bmatrix}^T$ is to be determined, and the matrices are properly partitioned. Eliminating $\ddot{X}_2$ in Eq. (29) yields

$$(D_{11} - D_{12}D_{22}^{-1}D_{21})\ddot{X}_1 - (N_1 - D_{12}D_{22}^{-1}N_2) = R \begin{bmatrix} \tau_2 \\ \tau_3 \end{bmatrix} \tag{30}$$

where

$$R = \begin{bmatrix} -1 & 0 \\ 1 & -1 \end{bmatrix} - D_{12}D_{22}^{-1} \begin{bmatrix} 0 & 1 \\ 0 & 0 \\ 0 & 0 \end{bmatrix}. \tag{31}$$

The computed input torques in terms of known states are then substituted back into Eq. (29) in order to obtain the differential equation from which X_2 can be determined. The initial conditions associated with this differential equation should be set to the values of X_2 at takeoff.

The conditions imposed so far guarantee periodicity of the two interpolated coordinates in flight. Furthermore, the following conditions must be satisfied in any hopping cycle:

$$\begin{cases} \theta_3(t_{TD_n}) = \theta_3^{TD_{n-1}} \\ \dot{\theta}_3(t_{TD_n}) = (\dot{\theta}_3^{TD_{n-1}})^- \\ y_f(t_{TD_n}) = 0. \end{cases} \tag{32}$$

While a general solution for X_2 might not be periodic in the sense of a complete hopping cycle, it is next shown that it is possible to find initial conditions for which the solution is periodic.

Since the solution of a system of differential equations is continuously dependent on its initial conditions, a continuous mapping can be defined between the initial conditions and the value of the solution at any time; under certain circumstances, a fixed point of such mapping corresponds to a periodic solution. Since the number of initial conditions (six) exceeds the number of periodicity conditions (three), a periodic solution is guaranteed.

Analytical and numerical methods have been presented for finding fixed points of various mappings. Here, no analytical solution can be obtained to the system of differential equations (29), and they are numerically integrated. Also, it is emphasized that a fixed point, for this case, refers to any solution satisfying conditions (32). It should be mentioned that the ankle coordinate x_a does not affect the motion periodicity.

Finally, if impact at touchdown is to be avoided, two more constraints are imposed to Eqs. (32), which requires that the velocity of the trailing limb tip becomes zero just before touchdown:

$$\begin{cases} \dot{y}_f(t_{TD_n}) = 0 \\ \dot{x}_f(t_{TD_n}) = 0. \end{cases} \tag{33}$$

5. Simulation and Results

Computer simulation is performed using the presented synchronization control strategy in order to obtain repeatable hopping cycles for biped robots. The case robot consists of three links, namely, thigh, shank, and torso, and one degree of underactuation in ankle joint. The involved parameters of the robot and the initial conditions of its link-segmental model are given, respectively in Tables 1 and 2.

Table 1. Parameters of the simulated model.

Link	Mass (kg)	Moment of Inertia ($\mathrm{Kg \cdot m^2}$)	Length (m)	CoM Distance from Proximal Joint (m)
Shank	0.2	0.02	0.1	0.05
Thigh	0.2	0.02	0.1	0.05
Torso	0.5	0.1	0.1	0.03

Table 2. Initial conditions of the simulated model.

Link	Initial Position (rad)	Initial Velocity (rad/s)
Shank	0	5.6
Thigh	$-\pi/6$	-3.0
Torso	$\pi/8$	-1.0

For synchronization control, a linear SLIP system is considered with spring stiffness $k = 1000\,\mathrm{N/m}$. Other parameters of the mass spring system including the initial conditions are calculated according to the link-segmental biped parameters. Finally, the free length of the spring was set as below:

$$l_o = \begin{cases} \eta|_{t=0} & \alpha < 0 \text{ (recoil)} \\ \eta|_{t=0} + \delta l_0 & \alpha > 0 \text{ (rebound)} \end{cases}, \tag{34}$$

with $\delta l_0 = 0.002\,\mathrm{m}$.

The proportional-differential (PD) controller gains for stance control of biped hopping, defined in Sec. 4.1, are set as

$$K_p = 8, \quad K_d = 6. \tag{35}$$

The simulated hopping based on the presented control strategy, robot parameters, and the specified initial conditions is illustrated in Fig. 3. The straight and dashed lines show the biped motion during stance and flight, and the dots show the trajectory of biped center of mass.

A complete cycle of hopping takes about 0.22 sec with 75% in stance phase and 35% in flight phase. The hopping range per cycle is about 6 cm, and the hopping speed is 27.3 cm/sec.

From the animation of a complete hopping cycle shown in Fig. 3, it can be concluded that in stance phase, the ankle joint angle is increasing to roll the biped

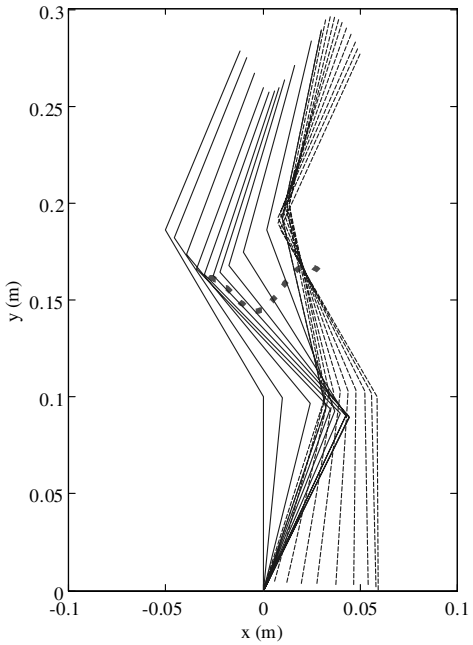

Fig. 3. Synchronization of the biped model with the corresponding SLIP model; The dots track the SLIP trajectory.

center of mass to the forward direction of hopping, and in the mean time, the flexion and the afterward extension of the ankle joint help the biped bounce back from the previous flight phase. The torso joint angle is dominated by the SLIP system, and is continuously decreasing.

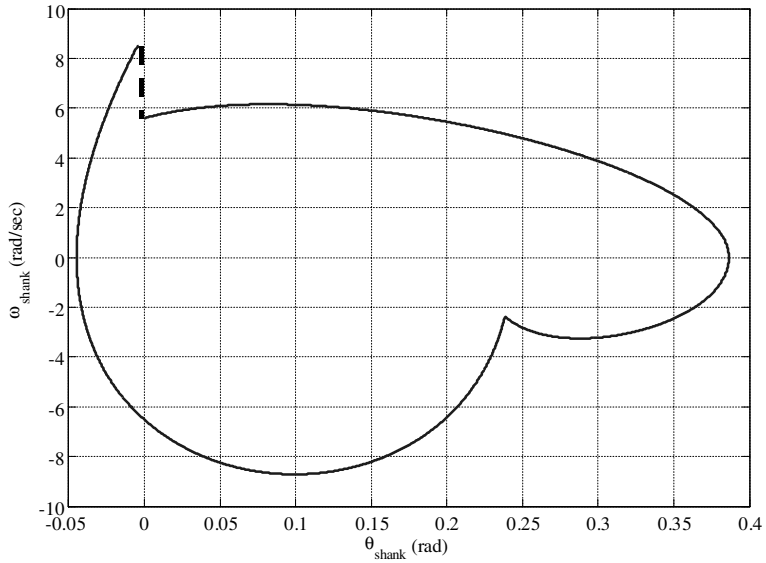

(a)

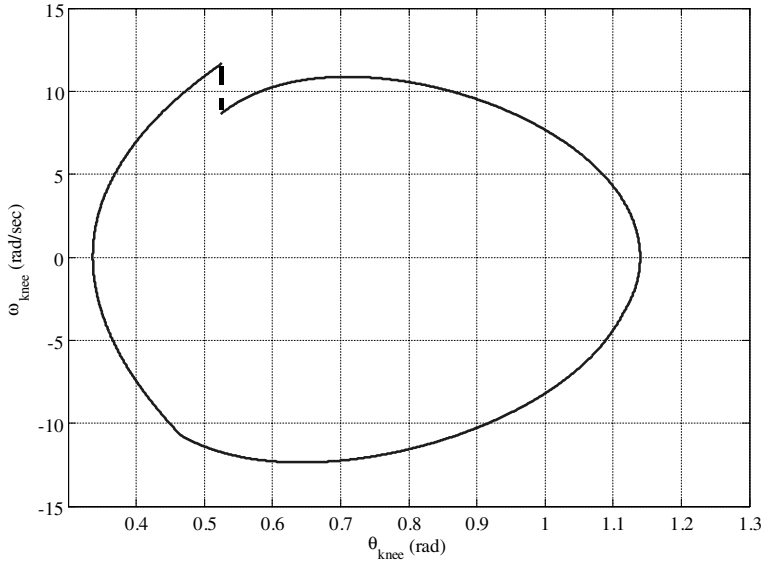

(b)

Fig. 4. Biped system: (a) shank, (b) thigh, (c) torso.

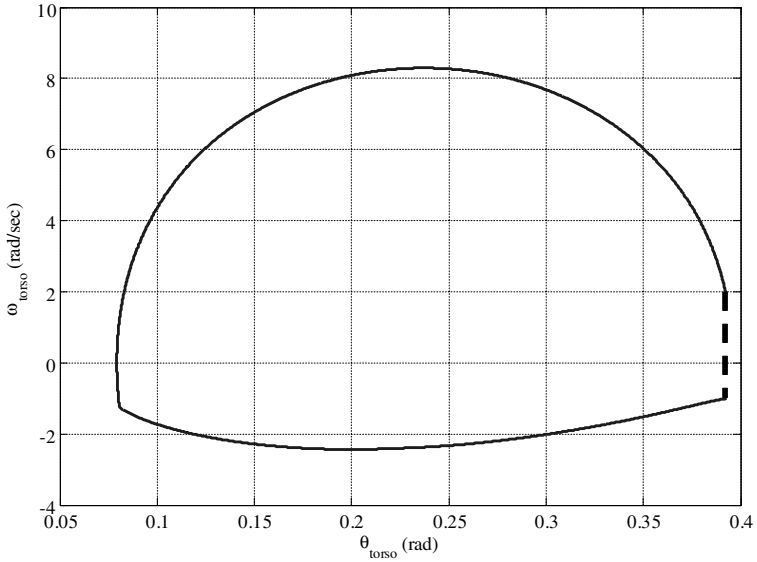

(c)

Fig. 4. (*Continued*)

Figures 4 and 5, respectively, show the joints phase plots and the corresponding mass spring states only during stance.

The main strategy of joint profiling in flight phase is to set the biped links at the landing stance to the same state as the initial ones, so that a repeatable hopping cycle is obtained. Sharp edges in Fig. 4 indicate the state of the biped at takeoff. Also, the dashed lines represent momentarily changes in velocities that happen due to impact.

As shown in Fig. 5, the SLIP system exhibits a smooth V-shaped length and monotonically increasing angle of attack.

The torques applied in knee and torso joints of the biped robot, calculated from the presented control strategy, are plotted in Fig. 6; the trend is dominated mostly by the angle extensions and flexions, and the sudden jump is because of the phase change. The only weak point is the large torques required to perform the desired hopping.

6. Conclusions

Experimental observations show that the complex, nonlinear dynamics of human fast locomotion can be represented by a simple spring mass system, namely Spring Loaded Inverted Pendulum (SLIP). This model, on the contrary to the other existing models, is originated in the elastic properties of muscles and tendons spanning the joints.

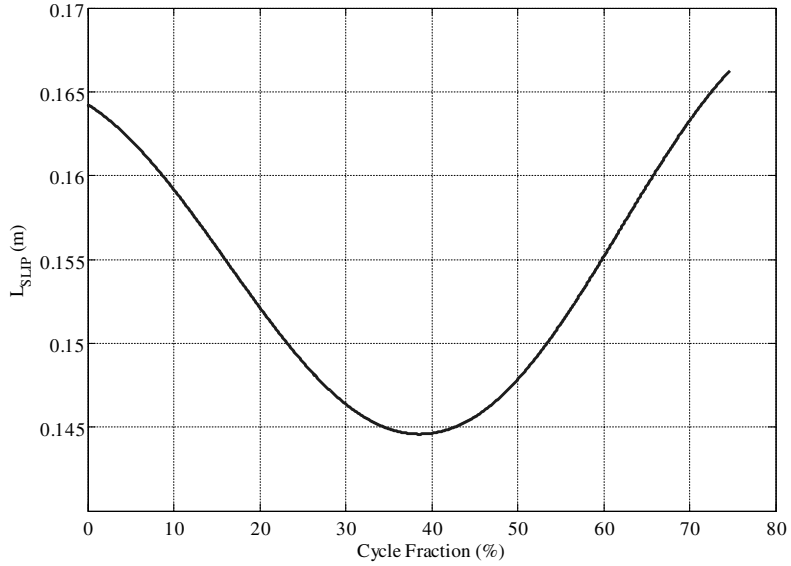

(a)

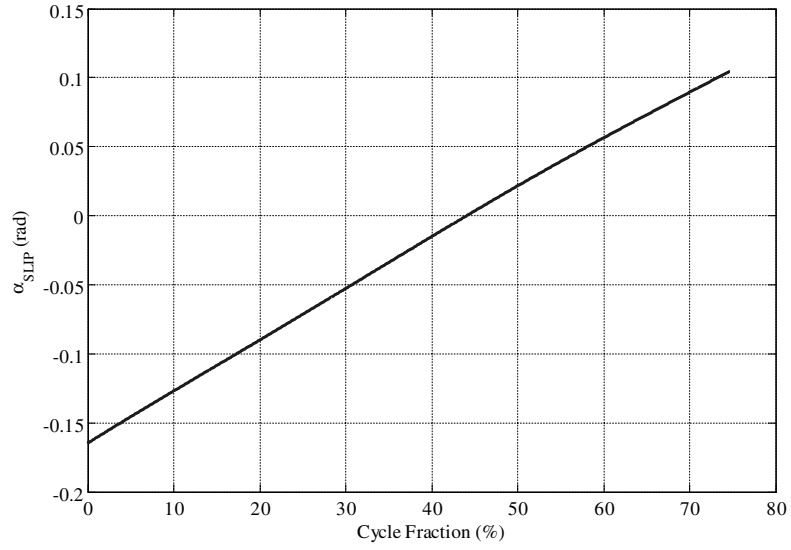

(b)

Fig. 5. Spring-mass system: (a) length, (b) angle of attack.

In this paper, a new approach to generating periodic joint trajectory and stable control of biped robots during fast locomotion is introduced. Inspired by the aforementioned observation, this method synchronizes the dynamics of link-segmental model with the SLIP representation of the biped. As a result, the biped center of

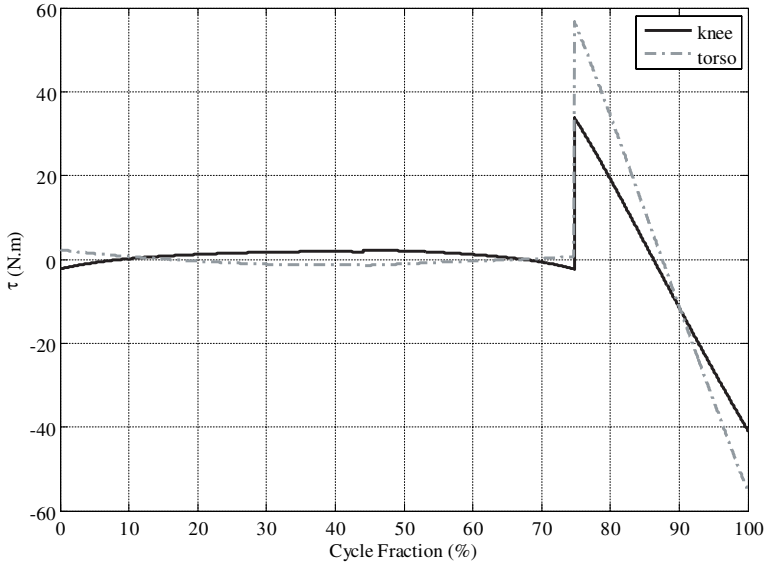

Fig. 6. Biped joint torques.

mass will dynamically and kinematically follow the trajectory of the mass in spring mass system, and the biped performs the desired locomotion.

As a case study, the biped robot is aimed to perform periodic hopping locomotion. Simulation is done on trajectory planning and control of a three-link biped robot with one degree of underactuation in ankle joint during hopping. In the stance phase, the synchronization control was accomplished by feedback linearization method and minimizing the error between the center of mass trajectory of two systems. During flight, biped dynamics is governed by gravity principle, but the trajectory is planned to guarantee periodic cycle of hopping.

Results show that the biped is capable of performing a complete periodic and stable hopping with remarkable average speed. The stance phase forms about 75% of the hopping cycle, while the rest is composed of takeoff, flight and landing. The phase plots evidently verify the periodicity of the motion, with the velocity discontinuities due to impact taken into account. Torques required by the presented control strategy are reasonable during stance, but become large to some extent due to the limited time of flight, during which the configuration of the robot has to reset back to the starting conditions of the next stance phase. It is expected that reducing the average speed would yield in lower torques that can be implemented on a real robot.

References

1. S. Kajita, F. Kanehiro, K. Kaneko, K. Fujiwara, K. Harada, K. Yokoi and H. Hirukawa, Resolved momentum control: Humanoid motion planning based on the

linear and anular momentum, in *IEEE/RSJ Int. Conf. on Intelligent Robots and Systems (IROS)*, Vol. 2 (IEEE Press, Las Vegas, USA, 2003), pp. 1644–1650.

2. S. Kajita, F. Kanehiro, K. Kaneko, K. Fujiwara, K. Harada, K. Yokoi and H. Hirukawa, Biped walking pattern generation by using preview control of zero-monment point, in *IEEE Int. Conf. on Robotics and Automation (ICRA)*, Vol. 2 (IEEE Press, Taipei, Taiwan, 2003), pp. 1620–1626.
3. J. Kuffner, S. Kagami, K. Nishiwaki, M. Inaba and H. Inoue, Dynamically-stable motion planning for humanoid robots, *Autonomous Robots* **12**(1) (2002) 105–118.
4. T. Sugihara, Y. Nakamura and H. Inoue, Realtime humanoid motion generation through zmp manipulation based on inverted pendulum control, in *IEEE Int. Conf. on Robotics and Automation (ICRA)* (IEEE Press, Taipei, Taiwan, 2003), pp. 1404–1409.
5. R. M. Alexander, Tendon elasticity and muscle function, *Comp. Biochem. Physiol. A* **133**(4) (2002) 1001–1011.
6. A. Seyfarth, A. Friedrichs, V. Wank and R. Blickhan, Dynamics of the long jump, *Biomechanics* (1999) 1259–1267.
7. C. T. Farley, J. Glasheen and T. A. McMahon, Running springs: speed and animal size, *Experimental Biology* **185** (1993) 71–86.
8. A. Seyfarth, H. Geyer, M. Gunther and R. Blickhan, A movement criterion for running, *Biomechanics* (2002) 649–655.
9. H. Geyer, A. Sayfarth and R. Blickhan, Spring-mass running: simple approximate solution and application to gait stability, *Theoretical Biology* **232**(3) (2005) 315–328
10. D. E. Koditschek, J. Robert and M. Buehler, Mechanical aspects of legged locomotion control, *Arthropod Structure & Development* (2004) 251–272.
11. W. J. Schwind, *Spring Loaded Inverted Pendulum Running: A Plant Model* (Dissertation, University of Michigan-Ann Arbor, 1998).
12. S. H. Tamaddoni, A. Alasty, A. Meghdari, S. Sohrabpour and H. Salarieh, Spring-mass jumping of underactuated biped robots, in *6th ASME Intl. Conf. on Multibody Systems, Nonlinear Dynamics, and Control (IDETC)* (IEEE Press, Las Vegas, USA, 2007).
13. A. Meghdari, S. Sohrabpour, D. Naderi, S. H. Tamaddoni, F. Jafari and H. Salarieh, A novel method of gait synthesis for bipedal fast locomotion, *Intelligent and Robotic Systems* **53**(2) (2008) 101–118.
14. A. Meghdari and M. Aryanpour, Dynamic modeling and analysis of the human jumping process, *Intelligent and Robotics Systems* **37** (2003) 97–115.
15. A. Seyfarth, H. Geyer and H. Herr, Swing-leg retraction: a simple control model for stable running, *Experimental Biology* **206**(15) (2003) 2547–2555.
16. S. H. Strogatz, *Nonlinear Dynamics and Chaos: With Applications to Physics, Biology, Chemistry, and Engineering* (Westview Press Cambridge, Massachusetts, 1994).

Seyed Hossein Tamaddoni received his B.S. and M.S. degrees in Mechanical Engineering from Sharif University of Technology in 2005 and 2007. During the last four years, he was a researcher at Center for Excellence in Design, Robotics, and Automation (CEDRA), and performed control and stability studies on Sharif Humanoid Robots, one of which participated in RoboCup 2005, Japan. His research interests include dynamics, control, robotics, and biomechanics of human locomotion. Seyed Hossein Tamaddoni is the author of two journal articles and several conference papers.

Farid Jafari received his B.S. and M.S. degrees from Sharif University of Technology (Tehran, Iran) in 2006 and 2008, respectively. From 2003 to 2008, he was Researcher at Center of Excellence in Design, Robotics and Automaton (CEDRA), and worked on two separate projects on designing and building a humanoid robot. Farid Jafari is the author of a journal paper and several conference papers. His research interests include dynamics, robotics, and control.

Ali Meghdari received his Ph.D. in Mechanical Engineering from the University of New Mexico in 1987. He then joined the robotics group of the Los Alamos National Laboratory (LANL) as a research collaborator. In 1988, he joined the Sharif University of Technology in Tehran as an Assistant Professor of Mechanical Engineering. In 1997, he was granted the rank of Full-Professor of Mechanical Engineering at S.U.T., and was recognized by the Iranian Society of Mechanical Engineers (ISME) as the youngest ME full-professor in Iran. During 1996–1999, he chaired the School of Mechanical Engineering at Sharif University of Technology. During 1993–94, he was a visiting research faculty at the AHMCT center of the University of California-Davis, and from 1999–2000, he served the IBDMS research center of the Colorado School of Mines, and the Rocky Mountain Musculoskeletal Research Laboratory (RMMRL) as a visiting research professor. Professor Meghdari has performed extensive research in the areas of robotics dynamics, flexible manipulators kinematics/dynamics, and dynamic modeling of biomechanical systems. He has published over 180 technical papers in refereed international journals and conferences, and has been the recipient of various scholarships and awards, the latest being: the 2001 Mechanical Engineering Distinguished Professorship Award from MSRT in Iran, and the 1997 ISESCO Award in Technology from Morocco. He was also nominated and elected as a Fellow of the ASME (American Society of Mechanical Engineers) in 2001. Since 2001, he has been the Vice-President of Academic Affairs, and the Director of Center of Excellence in Design, Robotics and Automation (CEDRA) at the Sharif University of Technology.

Saeed Sohrabpour received his M.S. and Ph.D. in Mechanical Engineering from the University of California-Berkeley in 1968 and 1971. He then joined the University of Shiraz in Iran as an Assistant Professor of Mechanical Engineering. From 1976 to 1977, he was a visiting research fellow at UCLA. In 1989, he joined Sharif University of Technology in Tehran as a Full-Professor of Mechanical Engineering. During 1990, he spent one year as a visiting professor at the University of New Mexico. Professor Sohrabpour has performed extensive research in the areas of large deformations, mechanics of metal forming, and optimal design of mechanical manipulators. Since 1997, he has been the President of Sharif University of Technology, and currently a fellow of the Academy of Sciences — Islamic Republic of Iran, and a member of Center of Excellence in Design, Robotics and Automation (CEDRA) at SUT.

View publication stats